



Flexural Behavior of Beams Reinforced with Hybrid Steel Rebars using Sea-Water Mixed concrete

Ahmed M. Ahmed^{1,2}, Magdy M.M. Genidi³, Ahmed Mohamed Elsherbeany⁴, Waleed Fouad Tawhed⁵

¹Assistant Professor of Department of Civil Engineering, Faculty of Engineering, Mataria, Helwan University, Cairo, Egypt

²Assistant Professor Civil and Construction Engineering Program, School of Engineering and Applied Science, Nile University, Giza, Egypt

³Associate Professor of Structural Engineering, Faculty of Engineering, Mataria, Helwan University, Cairo, Egypt

⁴MSc.Candidate Department of Civil Engineering, Faculty of Engineering, Mataria, Helwan University, Cairo, Egypt

⁵Associate Professor of Structural Engineering, Faculty of Engineering, Mataria, Helwan University, Cairo, Egypt

*Corresponding author E-mail: ahmedelsherbeany2033@gmail.com

Abstract.

This research investigates the potential of using seawater as a substitute for freshwater in concrete production, given the growing concern that more than half of the world's population may face freshwater shortages by 2025. The construction industry, which consumes a significant amount of freshwater in concrete production, could potentially alleviate this burden by using seawater. This study presents an experimental analysis of the effect of hybrid steel rebar on reinforced concrete beams that incorporate fiber bars and use seawater in the concrete mixture. A total of thirteen flexural reinforced concrete beams were tested, with varied weight percentages of steel fiber (16%, 33%, 50%, and 100%) relative to the total bars. These beams were divided into five groups for comparative analysis. The results revealed that beams mixed with seawater and tested before exposure to seawater showed the best performance. Additionally, it was observed that the load-bearing capacity of beams cast and cured with freshwater and hybrid steel rebar was superior to those cast and cured with seawater or a mixture of seawater and freshwater. In recent years, the use of steel fiber has been increasingly validated for reinforcing concrete structures, including beams and slabs. This research aims to investigate the impact of fiber reinforcement, particularly the use of polymer reinforcement, on the strengthening of reinforced concrete (R.C.) beams when mixed with different types of water. The experimental data indicate that the load-bearing capacity of reinforced concrete beams decreased with the addition of steel fiber in varying volumes of glass fiber.

Keywords: Glass fiber, Sea Water, exposure the corrosion, flexure failure.

1. Introduction

The corrosion of reinforcing steel is a significant issue for reinforced concrete (RC) structures [1,2] exposed to aggressive environments, such as marine structures, bridges, and parking garages. Corrosion can lead to a loss of serviceability or even the failure of the structure's load-carrying capacity. Fiber Reinforced Polymer (FRP) composites [3], made of fibers embedded in a polymeric resin, offer an alternative to steel reinforcement in RC structures due to their noncorrosive properties. Additionally, FRP materials are nonmagnetic, have high tensile strength, and are lightweight, making them ideal for structural engineering applications. However, FRP rebars exhibit brittle structural behavior [4].

To address this limitation, the use of hybrid steel-FRP rebars has been proposed to enhance both the ductility and corrosion resistance of reinforcing bars [5]. While current research on hybrid steel reinforcement has primarily focused on flexural members, only a few studies have examined members under compressive loads, such as beams [6]. The application of FRP reinforcement in compression members is limited due to its low compressive strength, which is only 30%—60% of its tensile strength. Despite the advantages of hybrid steel in construction, there are also drawbacks and limitations. Hybrid steel, characterized by steel encased in glass fiber, is designed to enhance corrosion resistance and increase the yield strength of steel.

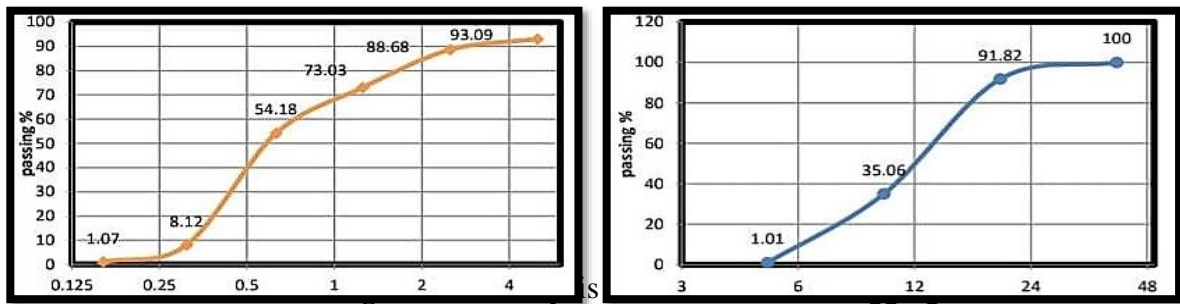
With the growing global population and the impact of climate change, the demand for resources, including freshwater, is becoming increasingly critical [7]. According to the World Meteorological Organization (WMO), by 2025, more than half of the world's population will face a shortage of drinking water [8]. In response to this impending crisis, the use of seawater in concrete production has gained attention, particularly in countries like the USA, United Kingdom, and Sweden. The global concrete industry requires billions of tons of freshwater annually for mixing, curing, and cleaning [9]. The authors advocate for the serious consideration of seawater as a mixing agent in concrete to conserve freshwater resources. Furthermore, the use of seawater in concrete production could be highly cost-effective [10], especially for coastal construction projects. However, most reinforced concrete standards currently prohibit the use of seawater due to the risk of early reinforcement corrosion caused by chloride (Cl) compounds present in seawater.

2. Materials and Methodology

2.1. Materials

The materials used to cast the specimens were made from locally available materials (sand, dolomite, sulfate resistant cement and drinking water and Sea Water). A mix was designed to reach target cubic compressive strength of 250 kg/m² after 28 days. Glass fiber bars Normal mild steel and high tensile steel reinforcement bars locally produced were used. Tests to determine the properties of these materials were carried out according to the Egyptian Standard Specifications. The obtained results were compared with the limits given in these specific generally. The nominal maximum size of the used gravel was 19 mm. Appendix grading of the gravel used. Cement: SRC, and Portland Sulphate Resisting Cement. Its appropriateness for concrete works is demonstrated by both the standard analysis and the physical attributes of the CEM IV/A (P) 42.5N-SR cement batches utilized in this study as established by the laboratory tests. Tests conducted on various cement batches made available for this study effort produced more or less comparable findings. This demonstrates the consistency of the utilized cement batches. It is in line with Egyptian requirements. Sand: The sand is

made of siliceous substances. It was without contaminants; the amount of silt, loam, and clay in it did not exceed 1% by weight. Additionally, they were free from anti-materials. In figure 1 we observe the sieve analysis for fine aggregate. Water: All of the mixtures were made with clean, impurity-free drinking water. seawater from red sea the values of water/cement ratios used were chosen and based on the total weight of water added to the air-dry materials as no allowance had been made for the absorption of mixing water by the aggregates (Dolomite): This research employed gravel that was siliceous. All of the used batches had acceptable quality. In figure 2 we observe the sieve analysis for fine aggregate Steel Reinforcement: Two definite types of steel used in beam 240 MPa for stirrups and on the other side 360 MPa used for longitudinal bars we are used to use different types of steel glass



2.2. Methodology

The experimental program was divided into two parts. Part (A) consisted of testing cubes and cylinders, while Part (B) involved testing 13 concrete beams, each with dimensions of 150 mm in width, 300 mm in thickness, and a total length of 2000 mm. All beams were subjected to centric loading. Twelve of the beams were reinforced with hybrid steel at varying percentages—16%, 33%, 50%, and 100% of the total bar diameter. The mixing water used for these beams was either freshwater or seawater, with different ratios. Table 1 provides the details of the reinforcement (RFT) for all specimen beams.

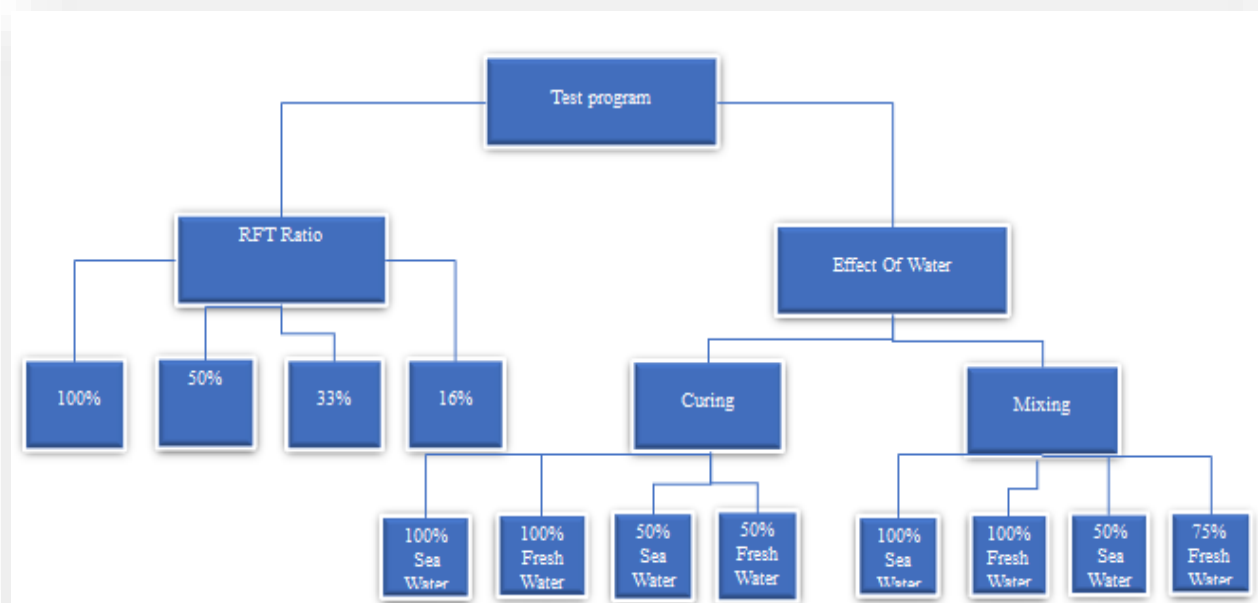


Fig 2. Main program test

2.2.1. Concrete mix

A concrete mix with a compressive strength of 25 MPa (using various water combinations—freshwater, seawater, 50% seawater/50% freshwater, 25% seawater/75% freshwater, and 75% seawater/25% freshwater) was used to cast all the tested concrete beams. Several trial mixes were conducted to determine the optimal mix proportions, which are presented in Table 1. The mix had a water-cement (w/c) ratio of 0.5, with a coarse aggregate of 10 mm maximum nominal size, and natural sand was used as the fine aggregate.

2.2.2. Compressive strength of concrete

Thirteen concrete mixes were considered in the study. five mixes were mixed and cured in Sea Water (SS), three concrete mixes were mixed with fresh water (FS) and cured in seawater, three concrete was mixed with 50% seawater and 50% fresh water (SFS) cured in Sea Water, three concrete was mixed with 25% seawater and 75% fresh water (SFS) cured in Sea Water, nine cylinder concrete mixes were mixed with 50% seawater and 50% fresh water (SFS) and cured in sea water, six cylinder concrete mixes were mixed with 75% seawater and 25% fresh water (SFS) and cured in seawater The concrete mixes were tested at ages of 7, 28 days for compression tests.

2.2.3. Test program

To investigate the above Figure, twelve beams casted with reinforced G-fiber while one concrete beam have only steel bars. The test program is organized into five groups, with each group comprising two types of beams:

- **Type 1:** Utilizes 5 bars of $\phi 10$ mm, encased in 2 mm glass fiber, alongside one beam with 5 bars of $\phi 12$ mm pure steel, and another beam with 5 bars of $\phi 10$ mm surrounded by 12 mm fiber.
- **Type 2:** Utilizes 5 bars of $\phi 6$ mm, encased in 6 mm glass fiber.
- **Type 3:** Utilizes 5 bars of $\phi 8$ mm, encased in 4 mm glass fiber.
- **Type 4:** Utilizes 5 bars of $\phi 6$ mm, encased in 6 mm glass fiber.
- **Type 5:** Utilizes 5 bars of $\phi 10$ mm, encased in 2 mm glass fiber.

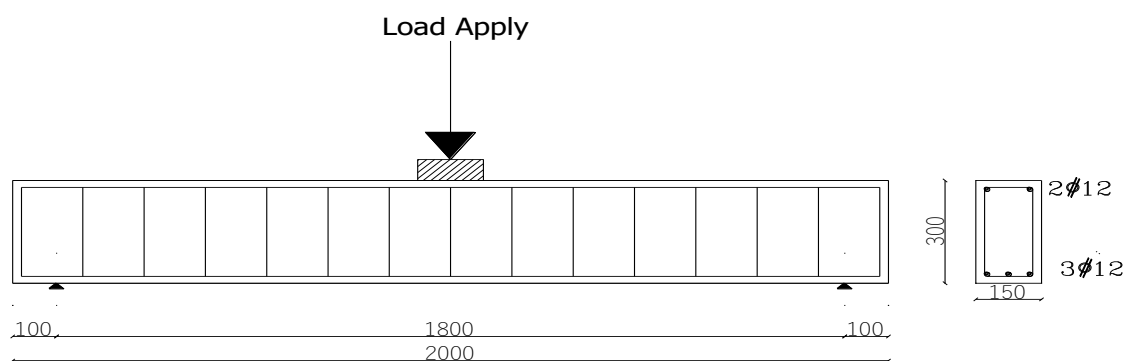


Fig 3. Beam reinforcement

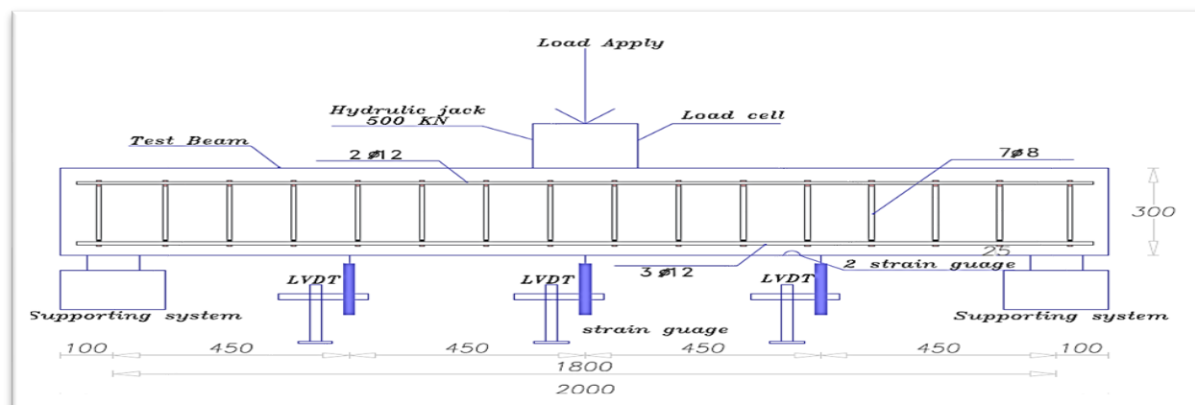


Fig 4. Test setup

Table 1. Details of specimen beam reinforcement

Group	Beam no.	Steel fiber S.f %	No. of RFT bars	Bar diameter	Thickness of hybrid steel in bars	Stirrups
1	B1	0.0%	12	12	0	7Ø8/m
	B2	100%	0	12	12	7Ø8/m
	B3	16%	10	12	2	7Ø8/m
	B4	33%	8	12	4	7Ø8/m
	B5	50%	6	12	6	7Ø8/m
2	B6	50%	6	12	6	7Ø8/m
	B7	16%	10	12	2	7Ø8/m
3	B8	50%	6	12	6	7Ø8/m
	B9	16%	10	12	2	7Ø8/m
4	B10	50%	6	12	6	7Ø8/m
	B11	16%	10	12	2	7Ø8/m
5	B12	50%	6	12	6	7Ø8/m
	B13	16%	10	12	2	7Ø8/m

3. Results and discussions

3.1. Compressive strength test

The obtained experiment results from material lab faculty of engineering Helwan university Materia branch as shown in Table 2 below, on the other side Brazilian test which is made in cylinders.

Table 2. 7& 28 days' compressive test

Number of cubes	Type of water in mixing	Failure load (kN) 7 days	Failure load (kN) 28 days	Stress kN/mm ² 7 days	Stress kN/mm ² 28 days
1	Sea water	278	475	158	269
2		253	487	143	276
2		288	499	163	283
3		269	459	153	260
2		278	487	158	276
3	75% sea water	283	539	160	307
1	25% fresh water	295	529	168	299
2	50% sea water	314	499	179	283
2	50% fresh water	347	501	198	284
2	25% sea water	326	533	185	311
3	75% fresh water	328	524	186	297
3	fresh water	318	498	181	282
2		322	488	183	276

3.2 Moment load in beams

Five Groups was examined into Concrete lab faculty of engineering Helwan university Materia branch, Cairo. The results as shown below, that is lead to calculate the ultimate load applied on each beam in five cases.

- in case of sea water (100%)
- in case of (25% fresh water & 75% sea water)
- in case of (50% fresh water & 50% sea water)
- in case of (75% fresh water & 25% sea water)
- in case of fresh water (100%)

Indicated that

B refer to: Beam number

GF refer to: Glass fiber ratio in parameter

FW refer to: Fresh water ratio in mixing

SW refer to: Sea water ratio in mixing

VF refer to: Volume of G-fiber from total bar diameter

3.2.1 Group one

3.2.1.1 Crack pattern and failure loads

The initial crack appeared at the bottom of the beam zone, accompanied by hairline cracks. All tested beams failed after the cracks propagated downward toward the loading region. The cracks were predominantly located in the bottom zones. Figure 4 illustrates the cracking and failure loads of the tested beams, while Figures 6, 7, 8, 9, and 10 show the cracking patterns for specimens B1, B2, B3, B4, and B, respectively.

relationship was linear for the five specimens only specimen number 5 Linear till the case of failure load was reached. We observe that max strain in upper quarter part of the RFT bar equal to 2003,9744,11891 and 7001 which founded into(B1-Gf0%-(0%Fw.100%Sw)), (B2-Gf100%-(0%Fw.100%Sw)), (B3-Gf16%-(0%Fw.100%Sw)), (B5-Gf50%-(0%Fw.100%Sw)). We observe that max strain equal to 14231 which found into (B4-Gf33%-(0%Fw.100%Sw)). Strain curves shown in Figure 10.

Table 3. Group (1) Cracking and failure loads

Group	Beam no	Cracking load p-crack (kN)	Failure stage		
			Failure load p-failure (kN)	Mode of failure	p-crack / p-failure
Group	B1-Gf0%-(0%Fw.100%Sw)	9.7	113.85	flexure failure	0.086
	B2-Gf100%-(0%Fw.100%Sw)	1.3	63	flexure failure	0.020
	B3-Gf16%-(0%Fw.100%Sw)	12	78	flexure failure	0.153
	B4-Gf33%-(0%Fw.100%Sw)	9.8	64	flexure failure	0.153
	B5-Gf50%-(0%Fw.100%Sw)	6.8	69.11	flexure failure	0.096

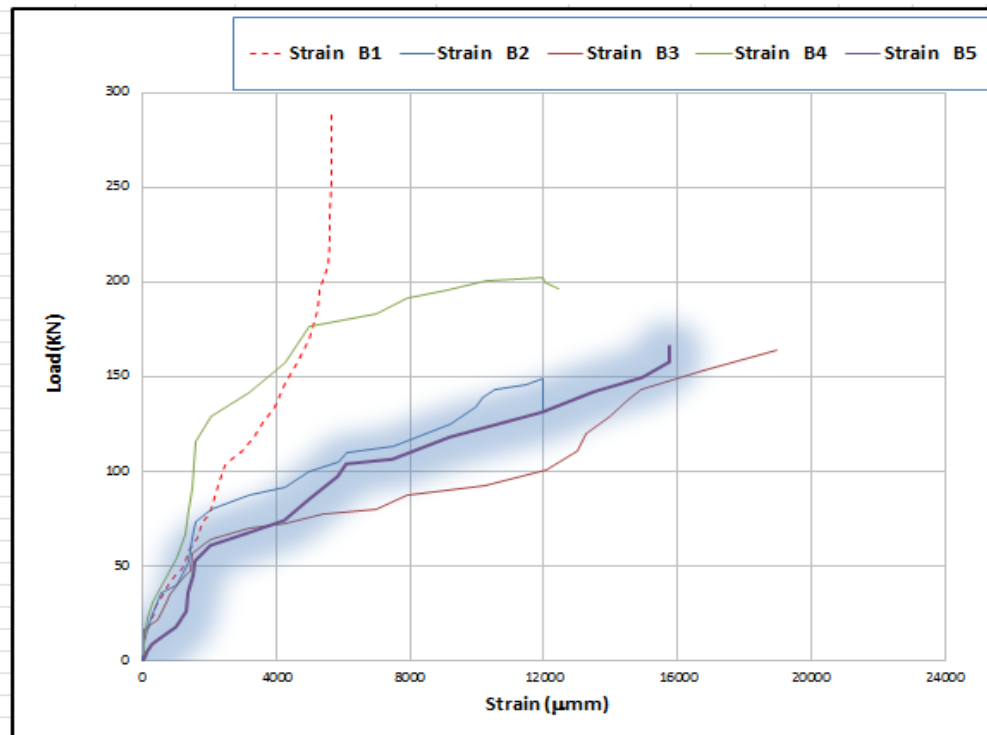


Fig 10. Strain for the group 1

3.2.2 Group two

3.2.2.1 Crack Patterns and Failure Loads

The first crack appeared either at the bottom of the beam zone, and some finer cracks appeared in the bottom, all tested beam failed after the propagation of cracks downwards to the loading region, and location of cracks was almost exclusively at the bottom zones Figure (12-13) shows the cracking patterns for tested beams in group 2 after failure. beam (B6-Gf 50%-(25%Fw.75%Sw).) containing volume fraction (V_f) = 50%, the first crack appeared at a load of about 22.7 kN. By increasing the load, more cracks appeared passing the upper quarter of the beam and the beam failed at load of about 166.31 kN beam (B7-Gf 16%-(25%Fw.75%Sw).) containing volume fraction (V_f) = 16%, the first crack appeared at a load of about 36.1 kN. By increasing the load, more cracks appeared passing the upper quarter of the beam and the beam failed at load of about 252.33 kN The failure crack patterns of the two tested beam (B6 and B7) were nearly similar, in that concentrated loads caused cracking and the major propagated through the bottom zone n loading area.

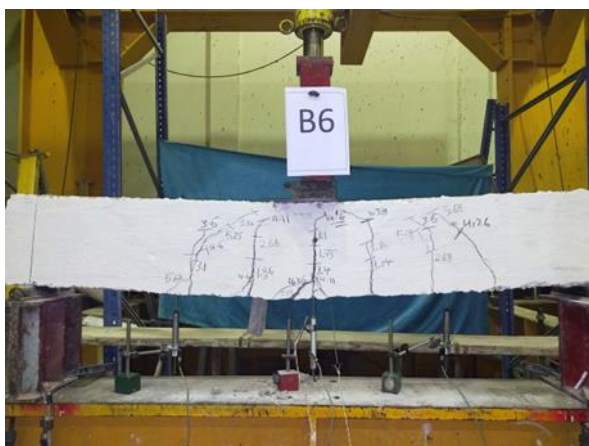


Fig 11. Crack pattern for B6

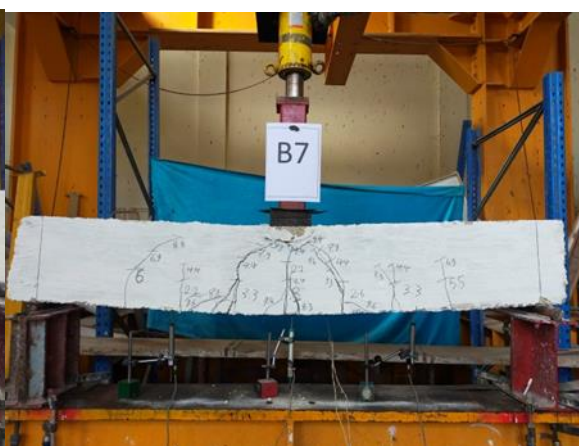


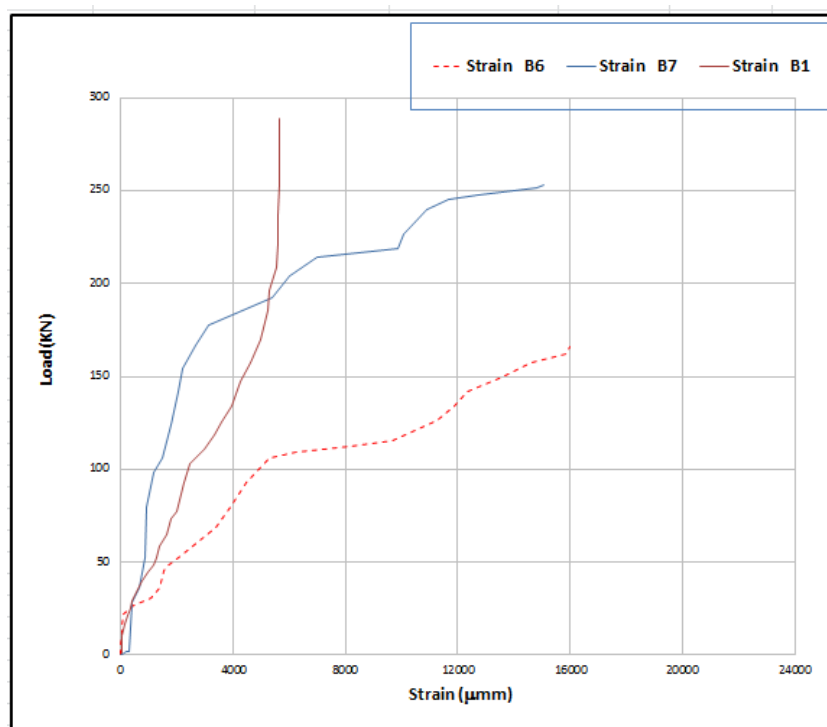
Fig 12. Crack pattern for B7

3.2.2.2 Measured Strain

The strain gauges were located in the mid height beam attached to the main reinforcing steel bars. From the results that observe that (B6-Gf 50%-(25%Fw.75%Sw)), (B7-Gf 16%-(25%Fw.75%Sw)). The relationship was linear for the two specimens. We observe that max strain in upper quarter part of the RFT bar equal to 9987 which founded into (B6-Gf 50%-(25%Fw.75%Sw)). We observe that max strain equal to 15086 which founded into (B7-Gf 16%-(25%Fw.75%Sw)), Strain curves shown in Figure 13.

Table 4. Cracking and failure loads

Group	Beam no	Cracking load(kN)	At Failure		
			P failure(kN)	Mode of failure	P Crack /P failure
Group 2	B6	22.7	166.31	flexure failure	.137
	B7	36.1	252.33	flexure failure	.143
Group 3	B8	23.41	177.87	flexure failure	.136
	B9	21	214.56	flexure failure	.098
Group 4	B10	24.19	241.61	flexure failure	.103
	B11	22.4	179.3	flexure failure	.123
Group 5	B12	35.2	257.64	flexure failure	.136
	B13	36	226.8	flexure failure	.159

**Fig 13.** Strain for the group 2.

3.2.3 Group three

3.2.3.1 Crack Patterns and Failure Loads

The first crack appeared either at the bottom of the beam zone, and some finer cracks appeared in the bottom, all tested beam failed after the propagation of cracks downwards to the loading region, and location of cracks was almost exclusively at the bottom zones

Figure (16-17) shows the cracking patterns for tested beams in group3 after failure.

beam (B8-Gf 50%-(50%Fw.50% SW).) containing volume fraction (V_f) = 50%, the first crack appeared at a load of about 23.41kN. By increasing the load, more cracks appeared passing the upper quarter of the beam and the beam failed at load of about 177.87 kN. beam (B9-Gf 16%-(50%Fw.50%Sw).) containing volume fraction (V_f) = 16%, the first crack appeared at a load of about 21kN. By increasing the load, more cracks appeared passing the upper quarter of the beam and the beam failed at load of about 214.56kN. The failure crack patterns of the two tested beam (B8 and B9) were nearly similar, in that concentrated loads caused cracking and the major propagated through the bottom zone n loading area concentrated loads caused cracking and the major propagated through the top zone n loading area experiments for Group one tested specimens.



Fig 14. Crack pattern for B8.

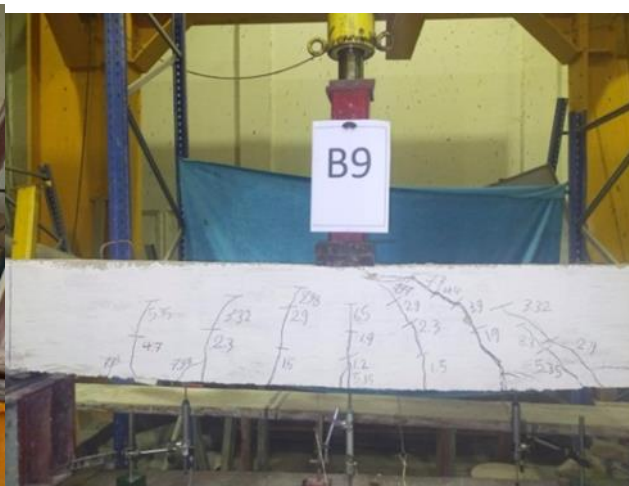


Fig 15. Crack pattern for B9.

3.2.3.2 Measured Strain

The strain gauges were located in the mid height beam attached to the main reinforcing steel bars. From the results that observe that (B8-Gf 50%-(50%Fw.50%Sw)), (B9-Gf 16%-(50%Fw.50%Sw)). The relationship was linear for the two specimens.

We observe that max strain in upper quarter part of the RFT bar equal to 10135 which founded into (B8-Gf 50%-(50%Fw.50%Sw)).

We observe that max strain equal to 2551 which founded into (B9-Gf 16%-(50%Fw.50%Sw)), Strain curves shown in Figure 16

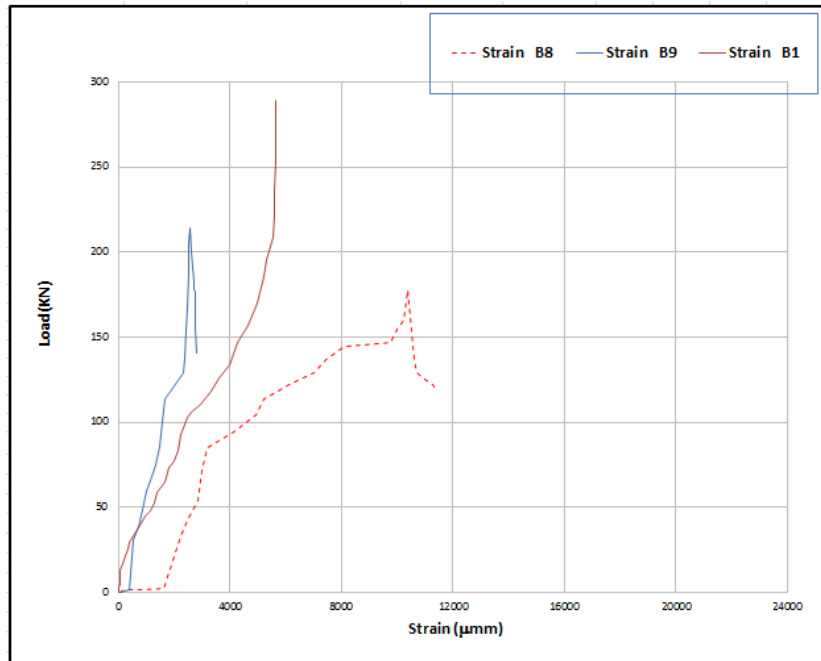


Fig 16. Strain for the group 3

3.2.4 Group four

3.2.4.1 Crack Patterns and Failure Loads

The first crack appeared either at the bottom of the beam zone, and some finer cracks appeared in the bottom, all tested beam failed after the propagation of cracks downwards to the loading region, and location of cracks was almost exclusively at the bottom zones. Figure (18-19) shows the cracking patterns for tested beams in group 4 after failure. beam (B10-Gf 50%-(75%Fw 25%Sw).) containing volume fraction (V_f) = 50%, the first crack appeared at a load of about 24.19 kN. By increasing the load, more cracks appeared passing the upper quarter of the beam and the beam failed at load of about 241.61 kN. beam (B11-Gf16%-(75%Fw.25%Sw).) containing volume fraction (V_f) = 16%, the first crack appeared at a load of about 22.4 kN. By increasing the load, more cracks appeared passing the upper quarter of the beam and the beam failed at load of about 179.3 kN. The failure crack patterns of the two tested beam (B10 and B11) were nearly similar, in that concentrated loads caused cracking and the major propagated through the bottom zone in loading area

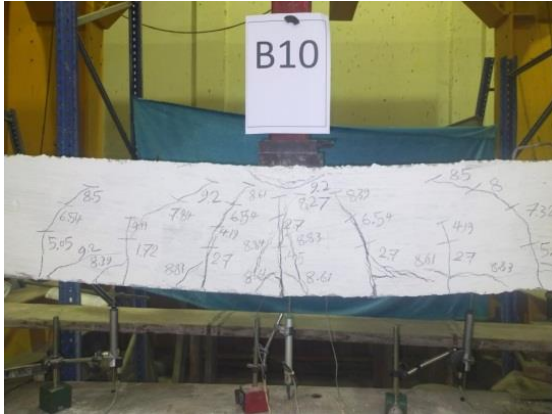


Fig 17. Crack pattern for B10

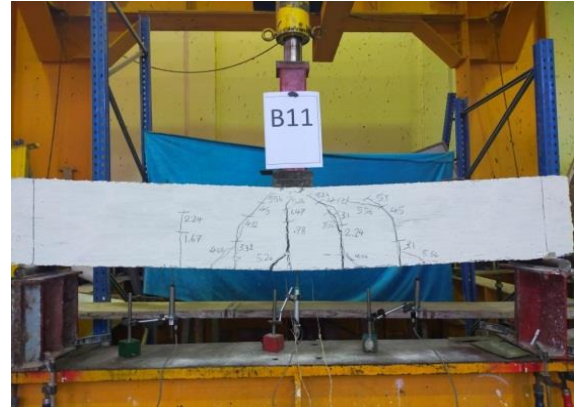


Fig 18. Crack pattern for B11

3.2.4.2 Measured Strain

The strain gauges were located in the mid height beam attached to the main reinforcing steel bars. From the results that observe that (B10-Gf 50%-(75%Fw 25%Sw)), (B11-Gf 16%-(75%Fw.25%Sw)). The relationship was linear for the two specimens. We observe that max strain in upper quarter part of the RFT bar equal to 14195 which founded into (B10-Gf 50%-(75%Fw 25%Sw)). We observe that max strain equal to 14201 which founded into (B11-Gf 16%-(75%Fw.25%Sw)), Strain curves shown in Figure 19.

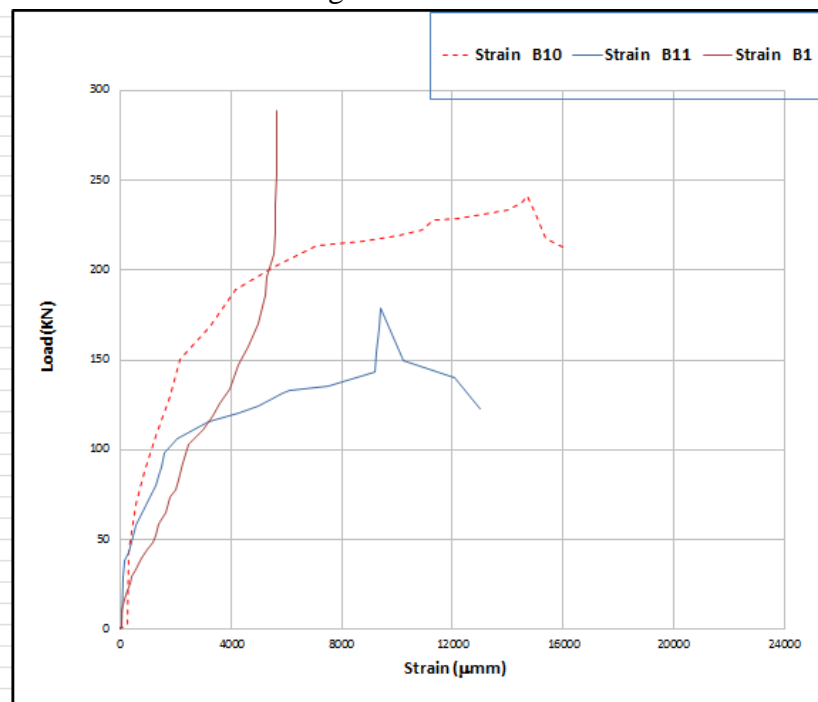


Fig 19. Strain for group 4.

3.2.5 Group five

3.2.5.1 Crack Patterns and Failure Loads

The first crack appeared either at the bottom of the beam zone, and some finer cracks appeared in the bottom, all tested beam failed after the propagation of cracks downwards to the loading region, and location of cracks was almost exclusively at the bottom zones

Figure (21-22) shows the cracking patterns for tested beams in group5 after failure.

beam (B12-Gf 50%-(100%Fw.0%Sw).) containing volume fraction (V_f) = 50%, the first crack appeared at a load of about 35.2 kN. By increasing the load, more cracks appeared passing the upper quarter of the beam and the beam failed at load of about 257.64 kN beam (B13-Gf 16%-(100%Fw.0%Sw).) containing volume fraction (V_f) = 16%, the first crack appeared at a load of about 36 kN. By increasing the load, more cracks appeared passing the upper quarter of the beam and the beam failed at load of about 226.8 kN. The failure crack patterns of the two tested beam (B12 and B13) were nearly similar, in that concentrated loads caused cracking and the major propagated through the bottom zone n loading area.



Fig 20. Crack pattern for B12.



Fig 21. Crack pattern for B13.

3.2.5.2 Measured Strain

The strain gauges were located in the mid height beam attached to the main reinforcing steel bars. From the results that observe that (B12-Gf 50%-(100%Fw.0%Sw)), (B13-Gf 16%-(100%Fw.0%Sw)). The relationship was linear for the two specimens. We observe that max strain in upper quarter part of the RFT bar equal to 14115 which founded into (B12-Gf 50%-(100%Fw.0%Sw)).

We observe that max strain equal to 17101 which founded into (B13-Gf 16%-(100%Fw.0%Sw)), Strain curves shown in Figure 22.

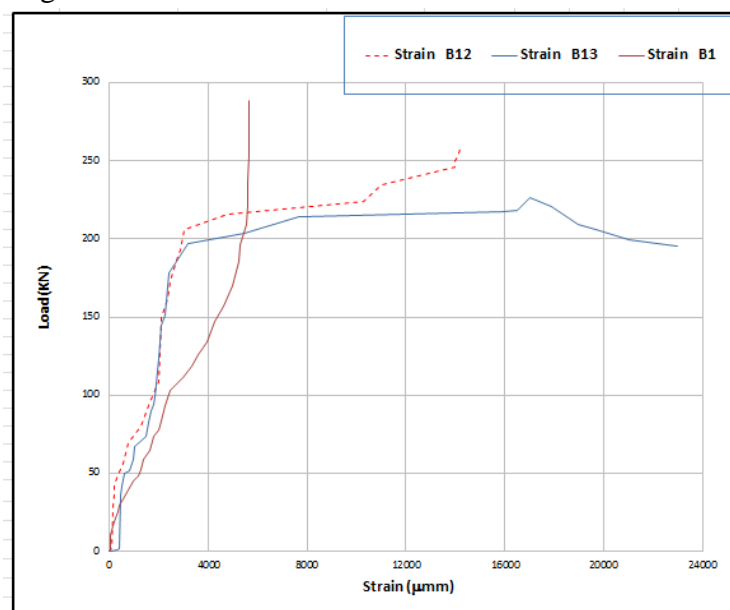


Fig 22. Strain for the group 5.

4. Conclusion

To conclude this manuscript, we provide some observations on utilizing seawater to enhance the flexural failure load behavior of hybrid reinforced concrete beams. This dissertation presents a novel approach to improving the flexural failure load of these beams, potentially offering an alternative to traditional methods. The proposed method involves incorporating varying percentages of seawater into the concrete mix before pouring it around the column, with different types of cement applied throughout the beam. In terms of crack patterns and modes of failure, all observed beam failures exhibit a vertical orientation.

References

- [1] El Fakhrany MH, el-Zamrawi A, Ibrahim W, Sherif A. Flexural performance of rapid-hardening concrete (RHC) beams with tension lap splice. *Beni-Suef University Journal of Basic and Applied Sciences* 2024;13:22. <https://doi.org/10.1186/s43088-024-00478-w>.
- [2] Elfakhrany MH, Zamrawi A, Ibrahim W, Sherif A. Experimental study on the mechanical properties and structural performance of the rapid hardening concrete. *Journal of Engineering and Applied Science* 2024;71:74. <https://doi.org/10.1186/s44147-024-00410-0>.
- [3] Fang S, Li L, Luo Z, Fang Z, Huang D, Liu F, et al. Novel FRP interlocking multi-spiral reinforced-seawater sea-sand concrete square columns with longitudinal hybrid FRP–steel bars: Monotonic and cyclic axial compressive behaviours. *Composite Structures* 2023;305:116487. <https://doi.org/https://doi.org/10.1016/j.compstruct.2022.116487>.
- [4] El fakhrany MH. Experimental study on the flexural behaviour of lap-spliced rapid hardening concrete beams. *Engineering Structures* 2024;313:118255. <https://doi.org/https://doi.org/10.1016/j.engstruct.2024.118255>.
- [5] Chaboki HR, Ghalehnovi M, Karimipour A, Brito J. Experimental study on the flexural behaviour and ductility ratio of steel fibres coarse recycled aggregate concrete beams. *Construction and Building Materials* 2018;2018. <https://doi.org/10.1016/j.conbuildmat.2018.07.132>.
- [6] Wang X, Chen Z, Ding L, Shi Y, Zhu Z, Wu Z. Long-term flexural behavior of concrete beams with hybrid FRP and steel reinforcements in simulated marine environment. *Structures*, vol. 33, Elsevier; 2021, p. 4556–67.
- [7] Zhang S, Gao D, Zhu H, Chen L, He Z, Yang L. Flexural behavior of seawater-mixed steel fiber reinforced concrete exposed to simulated marine environments. *Construction and Building Materials* 2023;373:130858.
- [8] Dong Z-Q, Wu G, Xu Y-Q. Bond and flexural behavior of sea sand concrete members reinforced with hybrid steel-composite bars presubjected to wet–dry cycles. *Journal of Composites for Construction* 2017;21:4016095.
- [9] Barkhordari Bafghi MA, Amini F, Safaye Nikoo H, Sarkardeh H. Effect of steel fiber and different environments on flexural behavior of reinforced concrete beams. *Applied Sciences* 2017;7:1011.
- [10] Xu W, Yang L, Gao D, Tang J, Sun G, Zhang Y. Mechanical properties of seawater-mixed steel fiber reinforced concrete. *Journal of Building Engineering* 2023;73:106823.